Buoyancy-Driven Radiative Unsteady Magnetohydrodynamic Heat Transfer over a Stretching Sheet with non-Uniform Heat Source/sink

D. Pal

Department of Mathematics, Visva-Bharati University,
Institute of Science, Santiniketan, West Bengal-731235, India.

Email: *dulalp123@rediffmail.com*

ABSTRACT

In the present study an unsteady mixed convection boundary layer flow of an electrically conducting fluid over an stretching permeable sheet in the presence of transverse magnetic field, thermal radiation and non-uniform heat source/sink effects is investigated. The unsteadiness in the flow and temperature fields is due to the time-dependent nature of the stretching velocity and the surface temperature. Both opposing and assisting flows are considered. The dimensionless governing ordinary non-linear differential equations are solved numerically by applying shooting method using Runge-Kutta-Fehlberg method. The effects of unsteadiness parameter, buoyancy parameter, thermal radiation, Eckert number, Prandtl number and non-uniform heat source/sink parameter on the flow and heat transfer characteristics are thoroughly examined. Comparisons of the present results with previously published results for the steady case are found to be excellent.

Keywords: Boundary layer flow; Stretching sheet; Magnetohydrodynamic; Thermal radiation; Mixed convection; Heat transfer.

NOMENCLATURE

a,b,c	empirical constants	T_∞	free-stream temperature
A^*	coefficients of space heat source/sink	t	time (s)
B^*	temperature-dependent heat source/sink	U_w	stretching surface velocity
B_0	magnetic field	V_w	mass suction/injection velocity
c_p	specific heat at constant pressure	u, v	x and y components of fluid velocity
C_f	local skin-friction coefficient	x	vertical or tangential distance
Ec	Eckert number	y	normal distance
$f(\eta)$	dimensionless stream function		
f_0	suction/injection parameter	α	unsteadiness parameter
g	acceleration due to gravity	β	thermal expansion coefficient
Gr_x	local Grashof number	η	similarity variable
K^*	mean absorption coefficient	κ	thermal conductivity
M	magnetic parameter	λ	mixed convection or buoyancy parameter
Nr	thermal radiation parameter		
Nu_x	local Nusselt number	μ	fluid dynamic viscosity
Pr	Prandtl number	ν	fluid kinematic viscosity
q'''	non-uniform heat source/sink	ρ	fluid density
q_r	radiative heat flux	ψ	stream function
q_w	local heat flux	σ	electric conductivity
Re_x	local Reynolds number	σ^*	Stephan-Boltzman constant
T	fluid temperature	$\theta(\eta)$	dimensionless temperature
T_w	wall temperature	τ_w	wall shear stress

1. INTRODUCTION

The problem of flow and heat transfer induced by continuous stretching heated surface is important as it has many practical applications in the manufacturing processes with obvious relevance to polymer extrusion, in which the extrudate emerges from a narrow slot. For instance, in a melt-spinning process, the extrudate from the die is generally drawn and simultaneously stretched into a filament or sheet, which is thereafter solidified through rapid quenching or gradual cooling by direct contact with water or chilled metal rolls. In fact, stretching will bring in an unidirectional orientation to the extrudate, thereby improving the quality of the final product considerably which greatly depends on the flow and heat transfer mechanisms. Glass blowing, wire drawing, continuous casting, and spinning of fibers also involve the flow due to a stretching surface. Tsou *et al.* (1967) considered the effect of heat transfer on a continuously moving surface with a constant velocity. Dutta *et al.* (1985) determined the temperature distribution in the flow over a stretching surface subject to uniform heat flux. Vajravelu and Hadjinicolaou (1997) studied flows and heat transfer characteristics in an electrically conducting fluid near an isothermal sheet. Ravindranath *et al.* (2010) discussed the combined effect of convective heat and mass transfer on hydromagnetic electrically conducting viscous, incompressible fluid through a porous medium in a vertical channel bounded by flat walls. Recently, Basiri Parsa *et al.* (2013) presented MHD boundary-layer flow over a stretching surface with internal heat generation or absorption.

All the above mentioned studies deal with stretching surface by considering flow to be steady. Not much attention has been given in the above studies when the stretching force and surface temperature are varying with time. Several authors (Na and Pop, 1996; Andersson *et al.*, 2000) studied the heat transfer in a liquid film on an unsteady stretching surface by using a similarity method to transform governing time-dependent boundary layer equations into a set of ordinary differential equations. Elbashbeshy and Bazid (2004) have presented similarity solutions of the boundary layer equations in the study of unsteady flow and heat transfer over an unsteady stretching sheet. Ishak *et al.* (2009a) analyzed the unsteady laminar boundary layer flow over a continuously stretching permeable surface with prescribed wall temperature. Xu and Liao (2005) presented an accurate series solution for an unsteady MHD flow of a non-Newtonian fluid over a non-impulsively stretch-

ing flat sheet. Ali and Magyari (2007) studied the unsteady fluid and heat flow induced by a submerged stretching surface while its steady motion is slowed down gradually.

A new dimension is added to the study of flow and heat transfer in a viscous fluid over a stretching surface by considering the effect of thermal radiation. The radiative effects have important applications in physics and engineering particularly, in the space technology and high temperature processes. But very little is known about the effects of thermal radiation on the boundary layer flows. Thermal radiation effects might play a significant role in controlling heat transfer process in polymer processing industry. The quality of the final product depends to a great extent on the heat controlling factors and the knowledge of radiative heat transfer in the system which leads to a desired product of sought characteristics. The effect of radiation on heat transfer problems have been studied by Hossain and Takhar (1996). The radiation effect on heat transfer of a micropolar fluid past a continuously moving plate was investigated by Raptis (1998). Pal and Malashetty (2008) have presented similarity solutions of the boundary layer equations to analyze the effects of thermal radiation on stagnation-point flow over a stretching sheet with internal heat generation or absorption. Pal (2009) investigated the effect of thermal radiation on heat and mass transfer in two-dimensional stagnation-point flow of an incompressible viscous fluid over a stretching sheet in the presence of buoyancy force. Recently, Pal and Mondal (2010) examined the effect of non-uniform heat source/sink and variable viscosity on MHD non-Darcy mixed convection heat transfer over a stretching sheet embedded in a porous medium in the presence of Ohmic dissipation. Srinivasacharya and Reddy (2013) investigated on mixed convection heat and mass transfer over a vertical plate in a Power-Law fluid-saturated porous medium with thermal radiation and chemical reaction effects. Recently, Poornima1 and Bhaskar Reddy (2013) studied the effects of thermal radiation and chemical reaction on magnetohydrodynamic free convective flow past a semi-infinite vertical porous moving plate.

Therefore, the aim of the present paper is to analyze the combined effects of viscous and Ohmic heating on MHD mixed convection flow of an electrically conducting incompressible viscous fluid over an unsteady vertical stretching permeable surface in the presence of non-uniform heat source/sink and thermal radiation. The stream function is defined differently (com-

pared to uniform stretching sheet case) in arriving at the non-linear ordinary differential equations. These non-linear equations along with the appropriate boundary conditions are then solved by employing a numerical shooting technique with Runge-Kutta-Fehlberg integration scheme to study the effect of unsteadiness on heat transfer in the laminar flow in a porous medium past a semi-infinite stretching sheet. The results of these studies are of great importance, for example in the prediction of skin-friction (or shear wall stress rate) as well as heat transfer rate over a stretching sheet which would find applications in technological and manufacturing industries such as polymer extrusion to obtain quality final product.

Fig. 1. Schematic diagram of the problem.

2. MATHEMATICAL FORMULATIONS

Consider an unsteady two-dimensional laminar mixed convection boundary layer flow due to stretching vertical permeable sheet in a quiescent viscous incompressible fluid which issues from a thin slit, as shown in Fig. 1. The abbreviations VBL and TBL mentioned in Fig. 1. mean velocity boundary layer and thermal boundary layer, respectively. It is assumed that for time $t < 0$ the fluid and heat flows are steady and at time $t = 0$, the sheet is impulsively stretched with the velocity $U_w(x,t)$ along the x-axis, keeping the origin fixed in the fluid of ambient temperature T_∞. The x-axis is taken along the stretching surface in the direction of the motion and the y-axis is perpendicular to the sheet in the outward direction towards the fluid of ambient temperature T_∞. The flow is assumed to be confined in a region $y > 0$. The flow is caused by the stretching of the sheet which moves in its own plane with the surface velocity $U_w(x,t) = ax/(1-ct)$, where a(stretching rate) and c are positive constants having dimension time $^{-1}$ (with $ct < 1, c \geq 0$). It is noted that the stretching rate $a/(1-ct)$ increases with time since $a > 0$.

In order to get the effect of temperature difference between the surface and the ambient fluid, we consider the non-uniform heat source/sink in the flow. The wall mass suction velocity is $V_w = V_w(x,t)$, which will be determined later. The flow is subject to a transverse uniform magnetic field of strength $\overrightarrow{B} = (0,B,0)$. Application of such a magnetic field stabilizes the boundary layer flow. The magnetic Reynolds number is assumed to be small so that the induced magnetic field is negligible. We also take the strength of the electric field due to polarization of the electric charges to be negligi-
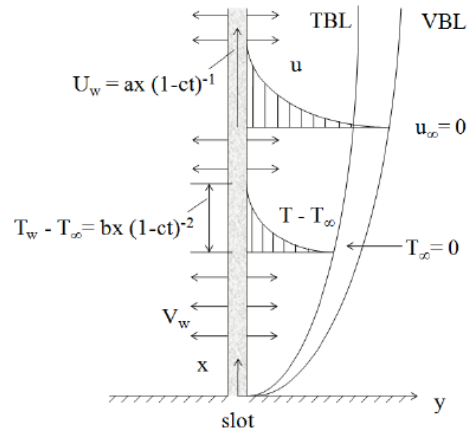
bly small. Under these assumptions along with the Boussinesq and boundary layer approximations, the governing unsteady basic boundary layer equations for momentum and heat transfer in the presence of thermal radiation and non-uniform source/sink may be written as

$$\frac{\partial u}{\partial x} + \frac{\partial v}{\partial y} = 0 , \tag{1}$$

$$\frac{\partial u}{\partial t} + u\frac{\partial u}{\partial x} + v\frac{\partial u}{\partial y} = \nu\frac{\partial^2 u}{\partial y^2} + g\beta(T - T_\infty) - \frac{\sigma B^2(t)}{\rho}u , \tag{2}$$

$$\frac{\partial T}{\partial t} + u\frac{\partial T}{\partial x} + v\frac{\partial T}{\partial y} = \frac{\kappa}{\rho c_p}\frac{\partial^2 T}{\partial y^2} + \frac{\nu}{c_p}\left(\frac{\partial u}{\partial y}\right)^2$$
$$- \frac{\sigma B^2(t)}{\rho c_p}u^2 - \frac{1}{\rho c_p}\frac{\partial q_r}{\partial y} + \frac{q'''}{\rho c_p} , \tag{3}$$

where u and v, respectively are the velocity components along $x-$ and $y-$ directions, t is the time, g is the acceleration due to gravity, β is the thermal expansion coefficient, σ and B_0 are the electric conductivity and magnetic field, respectively. T is the temperature inside the boundary layer, c_p is the specific heat at constant pressure, κ is the thermal conductivity, μ is the fluid viscosity, $\nu = \mu/\rho$ is the kinematics viscosity of the fluid and ρ is density of fluid and $B^2(t) = B_0^2(1 - ct)^{-1}$. Temperature of the stretching surface is $T_w(x,t)$, T_∞ is the temperature far away from the stretching surface with $T_w > T_\infty$ and $V_w = -(\nu U_w/x)^{1/2}f(0)$ represent the mass transfer at the surface with $V_w > 0$ for injection and $V_w < 0$ for suction (see Ishak *et al.*, 2009b).

The associated boundary conditions to the problem are

$$u = U_w(x,t), \quad v = V_w, \quad T = T_w(x,t) \quad at \quad y = 0 ,\text{(4)}$$

$$u \to 0, \quad T \to T_\infty \quad as \quad y \to \infty . \quad \text{(5)}$$

To transform the governing equations into a set of similarity equations, the following dimensionless parameters are introduced (see Fang *et al.*, 2009)

$$\Psi(x,y) = \left(\frac{\nu a}{1-ct}\right)^{\frac{1}{2}} x f(\eta) , \quad \text{(6)}$$

$$\eta = \sqrt{\frac{a}{\nu(1-ct)}} \, y , \quad \text{(7)}$$

where $\Psi(x,y,t))$ is the stream function defined as

$$u = \frac{\partial \Psi}{\partial y} = ax(1-ct)^{-1} f'(\eta) , \quad \text{(8)}$$

and

$$v = -\frac{\partial \Psi}{\partial x} = -\left[\nu a(1-ct)^{-1}\right]^{\frac{1}{2}} f(\eta) , \quad \text{(9)}$$

which identically satisfies the conservation of mass Eq. (1).

The non-uniform heat source/sink, q''' (Tsai *et al.*, 2008), is modelled as

$$q''' = \frac{\kappa U_w(x)}{x\nu}[A^*(T_w - T_\infty)e^{-\eta} + (T - T_\infty)B^*] ,\text{(10)}$$

where A^* and B^* are parameters of space-dependent and temperature-dependent heat generation/absorption, respectively. It is to be noted that the case $A^* > 0, B^* > 0$ corresponds to internal heat source and that $A^* < 0, B^* < 0$ corresponds to internal heat sink. It should be noted that when $t = 0$ (initial motion), Eqs. (2)-(4) describe the case of steady flow over a stretching sheet. The surface temperature of the sheet T_w is considered as a function of the distance x from the slot and time t in the form

$$T_w = T_\infty + \frac{bx}{(1-ct)^2} , \quad \text{(11)}$$

where b is constant with $b \geq 0$. Both heating $(T_w > T_\infty)$ and cooling $(T_w < T_\infty)$ of the sheet are considered, which correspond to assisting and opposing flows, respectively. The particular form of $U_w(x,t)$ and $T_w(x,t)$ presented in this paper has been chosen in order to devise a similarity transformation (see Ishak *et al.*, 2009a), which transform the governing partial differential equations (2)-(4) into a set of highly nonlinear ordinary differential equations.

The non-dimensional temperature is taken of the following form:

$$T(x,y) = T_\infty + \frac{bx}{(1-ct)^2}, \quad \theta(\eta) = \frac{T - T_\infty}{T_w - T_\infty}.\text{(12)}$$

It must be noted that the expressions (8) - (10), on which the analysis is based are valid only for $t < c^{-1}$.

By using Rosseland approximation, the radiative heat flux is given by

$$q_r = -\frac{4\sigma^*}{3K^*}\frac{\partial T^4}{\partial y} , \quad \text{(13)}$$

where σ^* and K^* are respectively the Stephan-Boltzman constant and the mean absorption coefficient. We assume the differences within the flow are such that T^4 can be expressed as a linear function of temperature. Expanding T^4 in a Taylor series about T_∞ and neglecting higher order terms thus,
$$T^4 \cong 4T_\infty T - 3T_\infty^4.$$

Substituting Eqs. (8)-(13) into (3) - (6), we obtain the following similarity equations

$$f''' + ff'' - f'^2 - \alpha\left(f' + \frac{1}{2}\eta f''\right) + \lambda\theta - Mf' = 0 , \quad \text{(14)}$$

$$\frac{1+Nr}{Pr}\theta'' - f'\theta + f\theta' - \alpha\left(2\theta + \frac{1}{2}\eta\theta'\right)$$
$$+ \frac{1}{Pr}(A^* f' + B^*\theta) + Ec\,(Mf'^2 + f''^2) = 0 , \quad \text{(15)}$$

where $Pr = \frac{\mu c_p}{\kappa}$ is the Prandtl number, $Nr = \frac{16\sigma^* T_\infty^3}{3K^*\kappa}$ is the thermal radiation parameter, $\alpha = \frac{c}{a}$ is a parameter that measures the unsteadiness. Further λ is the buoyancy or mixed convection parameter defined as $\lambda = Gr_x/Re_x^2$, in which $Gr_x = g\beta(T_w - T_\infty)x^3/\nu^2$ is the local Grashof number, $Ec = U_w^2/[c_p(T_w - T_\infty)]$ is the Eckert number, $M = \sigma B_0^2/(a\rho)$ is the magnetic parameter and $Re_x = U_w x/\nu$ is the local Reynolds number. It is to be noted that $\lambda > 0$ and $\lambda < 0$ correspond to assisting and opposing flows respectively, whereas $\lambda = 0$ is referred to the case of forced convection.

The boundary conditions (4)-(5) now become

$$f(0) = f_0, \quad f'(0) = 1, \quad \theta(0) = 1 , \quad \text{(16)}$$

$$f'(\infty) \to 0, \quad \theta(\infty) \to 0 , \quad \text{(17)}$$

where $f(0) = f_0$ with $f_0 < 0$ and $f_0 > 0$ corresponding to injection and suction, respectively.

In Eqs. (14) - (17), prime denotes derivative with respect to η. It is worth mentioning that the Eq. (15) reduces to Ishak *et al.* (2009a) as $Nr, A^*, B^* \to 0$.

The quantities of physical interest in this problem are the skin friction coefficient C_f and the local Nusselt number, Nu_x, which are defined as

$$C_f = \frac{\tau_w}{\rho U_w^2/2}, \qquad Nu_x = \frac{xq_w}{\kappa(T_w - T_\infty)}, \qquad (18)$$

where the wall shear stress τ_w and the surface heat flux q_w are given by

$$\tau_w = \mu\left(\frac{\partial u}{\partial y}\right)_{y=0}, \qquad q_w = -\kappa\left(\frac{\partial T}{\partial y}\right)_{y=0}, \quad (19)$$

with μ and κ being dynamic viscosity and thermal conductivity, respectively.

Using Eq. (19), quantity (18) can be expressed as

$$\frac{1}{2}C_f Re_x^{\frac{1}{2}} = f''(0), \qquad Nu_x/\sqrt{Re_x} = -\theta'(0). (20)$$

It is to be noted that the present problem reduces to steady-state flow in the absence of magnetic field, viscous and Ohmic dissipations, thermal radiation and non-uniform heat source/sink (i.e. $M = Ec = Nr = A^* = B^* = 0$) for $\alpha = 0$, then the closed-form solutions for velocity and temperature fields, in terms of Kummer's functions, are respectively given by (Ishak *et al.*, 2009a) as

$$f(\eta) = 1 - e^{-\eta}, \qquad (21)$$

$$\theta(\eta) = \frac{M(2, Pr+1, -Pr.e^{-\eta})}{M(2, Pr+1, Pr)}e^{(1-\eta-e^{-\eta})Pr}, (22)$$

where $M(a, b, z)$ denotes the confluent hypergeometric function (see Abramowitz and Stegun, 1965) as follows

$$M(a, b, z) = 1 + \sum_{n=1}^{\infty} \frac{a_n z^n}{b_n n!} \qquad (23)$$

where

$$a_n = a(a+1)(a+2)...(a+n-1),$$
$$b_n = b(b+1)(b+2)...(b+n-1). \qquad (24)$$

Thus using Eqs. (21) and (22), the skin friction coefficient $f''(0)$ and local Nusselt $-\theta'(0)$ are given by

$$f''(0) = -1, \qquad (25)$$

$$\theta'(0) = -\frac{2Pr}{1+Pr}\frac{M(3, Pr+2, Pr)}{M(2, Pr+1, Pr)}. \qquad (26)$$

3. THE METHOD OF SOLUTION

The coupled ordinary differential Eqs. (14) - (15) are of third order in f and second order in θ, which have been reduced to a system of five simultaneous equations of first-order for five unknowns. In order to solve this system of equations numerically we require five initial conditions but two initial conditions on f and one initial condition on θ are known. However, the values of f' and θ are known at $\eta \to \infty$. Thus, these two end conditions are utilized to produce two unknown initial conditions at $\eta = 0$ by using shooting technique. The most crucial factor of this scheme is to choose the appropriate finite value of η_∞. Thus to estimate the value of η_∞, we start with some initial guess value and solve the boundary value problem consisting of Eqs. (14) and (15) to obtain $f''(0)$ and $\theta'(0)$. The solution process is repeated with another large value of η_∞ until two successive values of $f''(0)$ and $\theta'(0)$ differ only after desired significant digit. The last value of η_∞ is taken as the finite value of the limit $\eta \to \infty$ for a particular set of physical parameters for determining velocity $f(\eta)$ and temperature $\theta(\eta)$ in the boundary layer. After knowing all the five initial conditions we solve this system of simultaneous equations using fifth-order Runge-Kutta-Fehlberg integration scheme. The value of η_∞ was selected to vary from 3 to 25 depending upon the physical parameters such as Prandtl number, non-uniform heat source/sink parameter, thermal radiation parameter and unsteadiness parameter so that no numerical oscillations would occur. The code was validated using the previously reported values (Grubka, Bobba, 1985; Ishak *et al.*, 2009a) and exact solutions (Ishak *et al.*, 2007) under some limiting cases. During the computation, the shooting error was controlled by keeping it to be less than 10^{-6}. Thus, the coupled nonlinear boundary value problem of third-order in f and second-order in θ has been reduced to a system of five simultaneous equations of first-order for

five unknowns as follows:

$$f_1' = f_2, \quad f_2' = f_3,$$

$$f_3' = -f_1 f_3 + f_2^2 + \alpha \left(f_2 + \frac{1}{2} \eta f_3 \right) - \lambda f_4 + M f_2,$$

$$f_4' = f_5,$$

$$f_5' = -\frac{Pr}{(1+Nr)} \left[f_1 f_5 - f_2 f_4 - \alpha \left(2 f_4 + \frac{1}{2} \eta f_5 \right) \right.$$

$$\left. + \frac{1}{Pr} (f_2 A^* + f_4 B^*) + Ec(M f_2^2 + f_3^2) \right],$$

(27)

where $f_1 = f$, $f_2 = f'$, $f_3 = f''$, $f_4 = \theta$, $f_5 = \theta'$ and a prime denotes differentiation with respect to η.

The boundary conditions now become

$$f_1 = 0, \quad f_2 = 0, \quad f_3 = \beta, \quad f_4 = 1,$$
$$f_5 = \gamma \qquad at \quad \eta = 0, \quad (28)$$
$$f_2 = 0, \quad f_4 = 0 \qquad as \quad \eta \to \infty. \quad (29)$$

Since $f_3(0)$ and $f_5(0)$ are not prescribed so we have to start with the initial approximations as $f_3(0) = \beta_0$ and $f_5(0) = \gamma_0$. Let β and γ be the correct values of $f_3(0)$ and $f_5(0)$, respectively. The resultant system of five ordinary differential equations is integrated using fifth-order Runge-Kutta-Fehlberg method and denote the values of f_3 and f_5 at $\eta = \eta_\infty$ by $f_3(\beta_0, \gamma_0, \eta_\infty)$ and $f_5(\beta_0, \gamma_0, \eta_\infty)$, respectively. Since f_3 and f_5 at $\eta = \eta_\infty$ are clearly function of β and γ, they are expanded in Taylor series around $\beta - \beta_0$ and $\gamma - \gamma_0$, respectively by retaining only the linear terms. The use of difference quotients is made for the derivatives appeared in these Taylor series expansions. Thus, after solving the system of Taylor series expansions for $\delta\beta = \beta - \beta_0$ and $\delta\gamma = \gamma - \gamma_0$, we obtain the new estimates $\beta_1 = \beta_0 + \delta\beta_0$ and $\gamma_1 = \gamma_0 + \delta\gamma_0$. Next the entire process is repeated starting with $f_1(0), f_2(0), \beta_1, f_4(0)$ and γ_1 as initial conditions. Iteration of the whole outlined process is repeated with the latest estimates of β and γ until prescribed boundary conditions are satisfied. Finally, $\beta_n = \beta_{n-1} + \delta\beta_{n-1}$ and $\gamma_n = \gamma_{n-1} + \delta\gamma_{n-1}$ for $n = 1, 2, 3, ...$ are obtained which seemed to be the most desired approximate initial values of $f_3(0)$ and $f_5(0)$. In this way all the five initial conditions are determined. Now it is possible to solve the resultant system of five simultaneous equations by fifth-order Runge-Kutta-Fehlberg integration scheme so that velocity and temperature fields for a particular set of physical parameters can easily be obtained. The results are provided in several tables and graphs.

4. DISCUSSION OF THE RESULTS

The transformed momentum and heat transfer equations (14) and (15) subject to the boundary conditions (16) and (17) for the flow of Newtonian fluid over a stretching sheet were approximated by a system of non-linear ordinary differential equations. These equations were solved numerically using Runge-Kutta-Fehlberg method with shooting technique. In order to verify the accuracy of the present numerical method, we have shown a comparison of the present results for skin friction coefficient with the exact solution when $f_0 = \alpha = A^* = B^* = \lambda = 0.0$ and results are tabulated in Table 1. Also, a comparison of the present results for wall temperature gradient $-\theta'(0)$ for $\alpha = 0.0, 1.0$ and for various values of Pr and λ with those of Grubka and Bobba (1985), Ishak et al. (2009a) and exact solution reported in Ishak et al. (2007), in the absence of non-uniform heat source/sink (i.e. $A^* = B^* = 0.0$) are tabulated in Table 2. From these Tables 1-2, it is noted that the comparisons are in excellent agreement with the previously published work which verifies the accuracy of the numerical method used in the present work.

It is also observed that the present results co-

Table 1 Comparison of skin friction coefficient $f''(0)$ for various values of Pr when $A^* = 0.0, B^* = 0.0$ with the exact solution

α	λ	Pr	Exact solution (Ishak *et al.*) (2007)	Present result
0.0	0.0	0.72	-1.000000	-1.000000
		1.0	-1.000000	-1.000000
		3.0	-1.000000	-1.000000
	1.0	1.0		-0.560752
	2.0			-0.177824
	3.0			0.176881
1.0	0.0			-1.320522
	1.0			-1.000835
	-0.5	10.0		-1.390258
	0.5			-1.251086

incides very well with the exact solution (Ishak et al., 2007). The slight deviation in the values may be due to the use of Runge-Kutta-Fehlberg method which has fifth order accuracy. This shows that the present results are very accurate. Further, the impact of some important physical parameters on skin friction coefficient $f''(0)$ and wall temperature gradient $-\theta'(0)$ may be analyzed from Table 1 and 2. It is to be noted that the effect of increasing the unsteadiness param-

eter, α, is to decrease the skin friction coefficient $f''(0)$ whereas the wall temperature gradient increases with unsteadiness parameter. It is also observed that the effect of buoyancy parameter λ is to increase the wall temperature gradient and the skin friction coefficient. Similarly the effect of Prandtl number is to increase the Nusselt number.

The combined effects of both Nr and Ec on temperature profiles are shown in the Fig. 2. It is observed from this figure that the effect of increasing the value of the thermal radiation parameter is to increase the temperature in the thermal boundary layer for both positive and negative values of the Eckert number far away from the stretching sheet. This is due to the fact that, the divergence of the radiative heat flux, $\partial q_r/\partial y$, as the Rosseland radiative absorptivity K^* decreases (see expression for Nr) which in turn increases the rate of radiative heat transfer to the fluid which causes the fluid temperature to increase. In view of this fact, the effect of thermal radiation becomes more significant as $Nr \to \infty$ and the radiation effects can be neglected when $Nr = 0$. It is found that in the absence of thermal radiation the temperature goes on decreasing towards negative temperature till it reaches to a minimum value in the boundary layer and thereafter the temperature starts increasing till it matches the boundary condition at $\eta = \infty$ for the case when the value of the Eckert number is negative. Similar behavior is seen when $Nr = 1.0$ but when $Nr = 2.0$ negative value of the temperature is not noticed instead all the values are found to be positive which shows that thermal radiation appreciably influence the temperature profiles when $Ec = -10$. Further, when $Ec = 10$ then there is formation of a peak temperature profile near the stretching sheet which decreases away from the sheet till it matches the boundary condition at $\eta = \infty$. The peak value of the temperature decreases with increase in the thermal radiation parameter Nr.

Figure 3 is aimed to shed light on the effect of the spatial-dependent internal heat generation/absorpion parameter A^* on the temperature distribution in the boundary layer for a fixed value of B^* for the case when $Ec = -2.0, 2.0$. It is observed from this figure that the temperature distribution in the boundary layer increases with increase in the values of A^* due to the fact that the presence of heat source $(A^* > 0)$ generates heat in the boundary layer which causes the temperature of the fluid to increase and reverse effect is seen when $(A^* < 0)$. The influence of the temperature-dependent internal heat
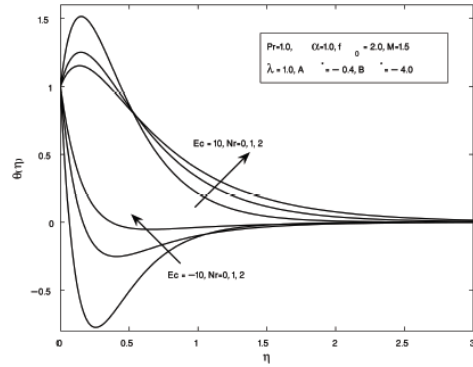

Fig. 2. Temperature profiles vs. η for various values of Nr and Ec in assisting flow.
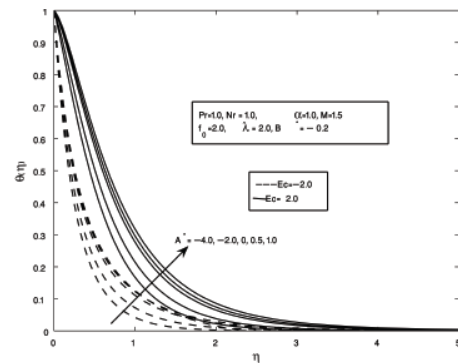

Fig. 3. Variation of temperature profiles with η for various values of A^* and Ec in assisting flow.
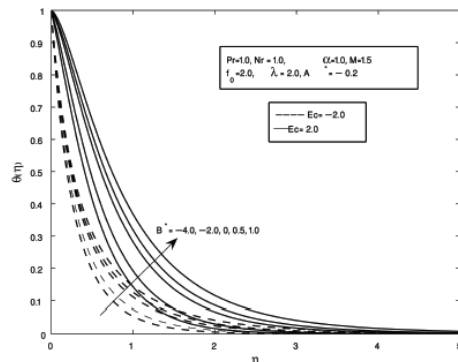

Fig. 4. Variation of temperature profiles with η for various values of B^* and Ec in assisting flow.

generation $(B^* > 0)$ or absorption $(B^* < 0)$ in the boundary layer on the temperature is similar to that of spatial-dependent internal heat generation or absorption is shown in the Fig. 4. Further, it is noted from this figure that the temperature decreases with increase in the heat absorption (sink) $(A^* < 0, B^* < 0)$ which is due to the fact that the thermal boundary layer thickness decreases with increase in the heat absorption (sink) $(B^* < 0)$ parameter. Further, it is

Table 2 Comparison of results of $-\theta'(0)$ at the wall with Grubka and Bobba (1985), Ishak *et al.* (2009b) and exact solution (Ishak *et al.*, 2007) for $A^* = B^* = 0.0$

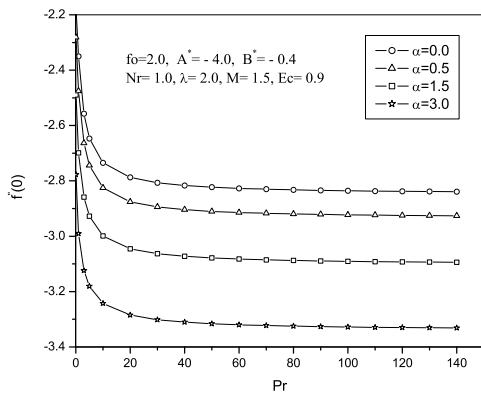| α	λ	Pr	Grubka and Bobba (1985)	Ishak *et al.* (2009b)	Exact sol. (Ishak *et al.*,2007)	Present results
0	0.0	0.72	0.8086	0.8086	0.808631350	0.80863135
		1.0	1.0000	1.0000	1.000000000	1.00000000
		3.0	1.9237	1.9237	1.923682594	1.92368256
		7.0	–	3.0723	3.072250207	3.07225020
		10.0	3.7207	3.7207	3.720673901	3.72067391
		100.0	12.294	12.2941	12.29408326	12.29408350
	1.0	1.0		1.0873		1.08727815
	2.0			1.1423		1.14233928
	3.0			1.1853		1.18529031
1	0.0			1.6820		1.68199253
	1.0			1.7039		1.70391283
	−0.5	10.0		5.5585		5.55850738
	0.5			5.5690		5.56899157

Fig. 5. Variation of skin friction coefficient profiles with *Pr* for various values of α in assisting flow.
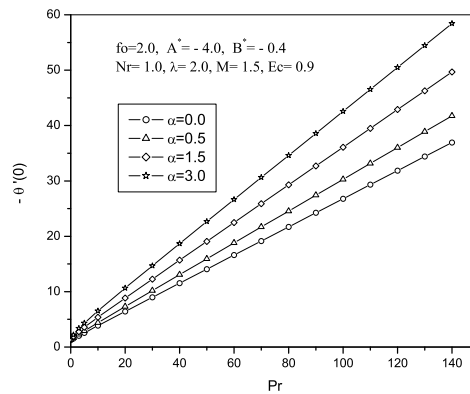

Fig. 6. Variation of Nusselt number profiles with *Pr* for various values of α in assisting flow.

observed that the boundary layer thickness increases as $B^* > 0$ increases which results in the higher value of temperature θ in the thermal boundary layer. The patterns of the temperature profiles in the boundary layer do not show any appreciable change though there is change in the values of the temperature in the boundary layer due to increase in the value of A^* or B^*.

The combined effects of the Prandtl number *Pr* and unsteady stretching parameter α on local skin friction coefficient and Nusselt number are shown in Figs. 5-6. From Fig. 5, it is observed that the local skin-friction coefficient $f''(0)$ decreases with increase in the Prandtl number for

all the values of α. Further $f''(0)$ decreases with the unsteady stretching parameter α keeping *Pr* fixed. Fig. 6 represents the behavior of the Prandtl number on the local Nusselt number $-\theta'(0)$. It is analyzed that the unsteady stretching parameter α increases the local Nusselt number and similar behavior is seen in the case of increasing the value of the Prandtl number. Figs. 7-8, respectively show the variation of local skin-friction coefficient and local Nusselt number against A^* for different stretching parameter α. It is seen that increasing the unsteady stretching parameter α decreases the local skin-friction coefficient whereas its effect is to increase the local Nusselt number for all the
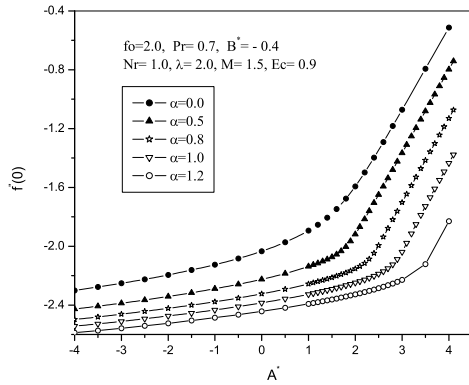
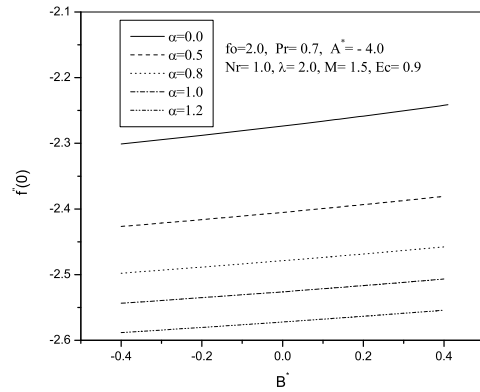**Fig. 7. Variation of skin friction coefficient profiles with A^* for various values of α in assisting flow.**

Fig. 8. Variation of Nusselt number profiles with A^* for various values of α in assisting flow.

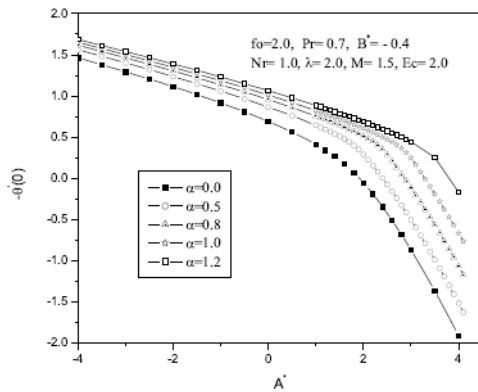**Fig. 9. Skin-friction coefficient profiles with B^* for various values of α in assisting flow.**
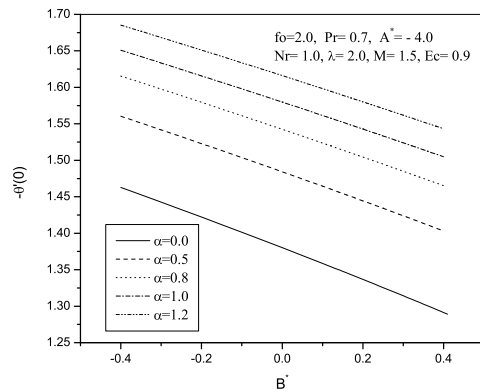

Fig. 10. Nusselt number profiles with B^* for various values of α in assisting flow.

values of A^*. Further, it is also seen that the skin-friction coefficient increases with increasing the value of A^* whereas opposite effect of A^* is seen on the local Nusselt number for all the values of α. Fig. 9. depicts the variation of skin-friction coefficient with B^* for various values of α. It is noted from this figure that the local skin-friction coefficient increases with increasing the values of B^* whereas reverse effect is seen by increasing the value of α. From Fig. 10. it is observed that the effect of increasing the value of B^* is to decrease the value of local Nusselt number whereas opposite trend is seen by increasing the values of α.

5. CONCLUSION

The present work deals with studying heat and mass transfer in the laminar flow of an electrically conducting fluid past an unsteady permeable stretching surface in the presence of the transverse magnetic field and thermal radiation with non-uniform heat source/ sink. The ef-

fects of various physical parameters on the heat transfer characteristics were examined. Numerical computations show that the present values of skin friction coefficient and local Nusselt number are in close agreement with those obtained by previous investigators in the absence of suction/injection, non-uniform heat generation/absorption and unsteadiness parameter. In the light of the present investigation, following conclusions are drawn:

(*i*) Viscous dissipation increases the temperature as it works like a heat source.

(*ii*) Velocity profiles increases in the assisting flow whereas reverse effect is observed in the opposing flow for both the values of $Ec = -3, 3$.

(*iii*) Increasing the thermal radiation parameter leads to increase in the value of the temperature profiles for both the values of $Ec = -10,\ 10$.

(*iv*) Temperature profiles increase with increasing the values of the space-dependent and temperature-dependent heat source parameter whereas reverse effect is seen by in-

creasing the space-dependent and temperature-dependent heat sink parameter. (*v*) Skin-friction coefficient decreases with increase in the unsteadiness parameter against Pr, A^* and B^*.

(*vi*) Nusselt number decreases due to increase in the unsteady stretching rate parameter when variations are observed against both temperature-dependent and space-dependent heat generation/absorption parameters.

REFERENCES

Abramowitz, M. and I. A. Stegun (1965). *Handbook of Mathematical Functions,* Dover, New York.

Ali, M. E. and E. Magyari (2007). Unsteady fluid and heat flow induced by a submerged stretching surface while its steady motion is slow down gradually. *Int. J. Heat Mass Transf 50*, 188–195.

Andersson, H. I., J. B. Aarseth and B. S. Dandapat (2000). Heat transfer in a liquid film on an unsteady stretching surface. *Int. J. Heat Mass Transf 43*, 69–74.

Basiri Parsa A., M. M. Rashidi and T. Hayat (2013). MHD boundary-layer flow over a stretching surface with internal heat generation or absorption. *Heat Trans Asian Res 42*(6), 500-514.

Dutta, B. K., P. Roy and A. S. Gupta (1985). Temperature field in flow over a stretching sheet with uniform heat flux. *Int. Comm. Heat Mass Transf 28*, 1234–1237.

Elbashbeshy, E. M. A. and M. A. A. Bazid (2004). Heat transfer over an unsteady stretching surface. *Heat Mass Transf 41*, 1-4.

Fang, T., J. Zhang and S. Yao (2009). Viscous flow over an usteady shrinking sheet with mass transfer, Chin. Phys. *Phys. Lett 26*, 0147031-0147034.

Grubka, L. J. and K. M. Bobba (1985). Heat transfer characteristics of a continuous stretching surface with variable temperature. *ASME J. Heat Transf. 107*, 248–250.

Hossain, M. A. and H. S. Takhar (1996). Radiation effect on mixed convection along a vertical plate with uniform surface temperature. *Int. J. Heat Mass Transf 31*, 243-248.

Ishak, A., R. Nazar and I. Pop (2007). Mixed convection on the stagnation point flow towards a vertical, continuously stretch-ing sheet. *ASME J Heat Transf 129*, 1087-1090.

Ishak, A., R. Nazar and I. Pop (2009a). Boundary layer flow and heat transfer over an unsteady stretching vertical. *surface. Meccanica 44:* 369-375.

Ishak, A., R. Nazar and I. Pop (2009b). Heat transfer over an unsteady stretching permeable surface with prescribed wall temperature. *Nonlinear Analysis: Real World Appls 10*, 2909–2913.

Na, T. Y. and I. Pop (1996). Unsteady flow past a stretching sheet. *Mech. Res. Commun. 23*, 413–422.

Pal, D. and M. S. Malashetty (2008). Radiation effects on stagnation-point flow over a stretching sheet with internal heat generation or absorption. *Int. J. Appl. Mech. Engg 13*, 427-439.

Pal, D. (2009). Heat and mass transfer in stagnation-point flow towards a stretching surface in the presence of buoyancy force and thermal radiation. *Meccanica 44*, 145–158.

Pal, D. and H. Mondal (2010). Effect of variable viscosity on MHD non-Darcy mixed convection heat transfer over a stretching sheet embedded in a porous medium with non-uniform heat source/sink. *Commun. Nonlinear Sci. Numer. Simul. 15*, 1553–1564.

Raptis, A. (1998). Flow of a micropolar fluid past a continuously moving plate by the presence of radiation. *Int. J. Heat Mass Transf. 41*, 2865–2866.

Poornima T. and N. Bhaskar Reddy (2013). Effects of thermal radiation and chemical reaction on mhd free convective flow past a semi-infinite vertical porous moving plate. *Int. J. of Appl. Math and Mech. 9*(7), 23-46.

Ravindranath, P., P. M. V. Prasad and D. R. V. Prasad Rao (2010). Computational hydromagnetic mixed convective heat and mass transsfer through a porous medium in a non-uniformly heated vertical channel with heat source and dissipation. *Computers and Mathematics with Appls. 59*, 803-811.

Srinivasacharya D. and G. Swamy Reddy (2013). Mixed convection heat and mass transfer over a vertical plate in a power-law fluid-saturated porous medium with radiation and chemical reaction effects. *Heat Trans Asian Res. 42*(6), 485-499.

Tsai R., K. H. Huang and J. S. Huang (2008). Flow and heat transfer over an unsteady stretching surface with non-uniform heat source. Int. Commun. *Int. Commun. Heat and Mass Transfer. 35*(10):13401343.

Tsou, F. K., F. M. Sparrow and R. J. Goldstein (1967). Flow and heat transfer in the boundary layer on a continuous moving surface. *Int. J. Heat Mass Transf. 10*, 219–235.

Vajravelu, K. and A. Hadjinicolaou (1997). Convective heat transfer in an electrically conducting fluid at a stretching surface with uniform free stream. *Int. J. Engg. Sci. 35*, 1237–44.

Xu, H. and S. J. Liao (2005). Analytic solutions of magnetohydrodynamic flows of non- Newtonian fluids caused by an impulsively stretching plate. *Journal of Non-Newton Fluid Mechanics 159*, 46–55.